

Modern magnetic field sensors – a review

Abstract. The paper presents a review on modern magnetic field sensors. After general remarks describing performances of magnetic field sensors the most important sensors are presented. In all cases the principle of operation, advantages and drawbacks and properties are discussed. Following sensors are presented – induction sensors, fluxgate sensors, magnetoresistive sensors (AMR sensors, spin valve sensors, magnetic tunnel junction sensors), Hall effect sensors, SQUID sensors, resonance sensors (NMR resonance, ESR resonance, Overhauser resonance). Other sensors as giant magnetoimpedance sensors, extraordinary MR sensors, magneto-optical sensors, MEMS sensor are also briefly described.

Streszczenie. Artykuł przedstawia przegląd najczęściej używanych czujników pola magnetycznego. W każdym przypadku przedstawiona zasada działania, wady i zalety oraz właściwości. Następujące czujniki są analizowane: czujniki indukcyjne, czujniki transduktorowe, czujniki magnetoimpedancyjne (AMR, GMR i tunelowe), hallotrony, SQUID, czujniki rezonansowe (NMR, ESR i Overhauser). Dodatkowo krótko opisano czujniki magnetoimpedancyjne, czujniki EMR (extraordinary magnetoresistance, czujniki magnetoptyczne i czujniki MEMS. (Czujniki pola magnetycznego)

Keywords: magnetic field sensors, induction coil sensors, fluxgate sensors, MR sensors, SQUID, Hall effect sensors

Słowa kluczowe: czujniki pola magnetycznego, czujniki indukcyjne, czujniki transduktorowe, czujniki magnetoimpedancyjne, SQUID

Introductory remarks

It should be noted that term “magnetic field sensor¹” does not mean that the sensor is used to magnetic field detection or measurement. For example only very small part of Hall sensors are used to magnetic field measurements – main part is used to mechanical measurement (proximity sensors, sensors in brushless motors etc). Similarly magnetoresistive sensor are mainly used as reading heads.

An more – because market for magnetic field sensors is rather narrow only these sensors have been developed which could be used in other area of applications. The SQUID sensors are mainly used in biomagnetic applications, flux-gate sensors are used in military industry, inductive sensors in geomagnetic research, resonance principle in medicine etc. Especially much luck had MR sensors due to application in rich computer industry.

compared we can conclude that from long time the situation is very stable and four main sensors are dominating. For very small magnetic field are used SQUID sensors, for small magnetic fields flux-gate sensors, for medium values are used MR sensors and for high magnetic field Hall sensors (Fig. 1). New principles and new sensors (for example GMI – giant magnetoimpedance sensors, magneto-transistors, magneto-optical sensors, extraordinary magneto-resistance, tunnel magnetoresistance TMJ) are still not competitive to well established four main principles. Of course old principles are also in progress but it is mainly miniaturization or improvement of parameters.

When we compare various sensor different parameters can be considered – sensitivity, linearity, range, frequency bandwidth, dimensions. Important is range of measured magnetic field and especially the smallest value of measured field. The upper limit is not so important because many magnetic sensors operate in magnetic feedback (Fig. 2). In this case these sensors are only zero field detectors and theoretically upper limit can be very large. We should also note that if sensors are used in magnetic feedback their linearity error is also suppressed. That is why many sensors, as for example AMR sensor, SQUID sensors or fluxgate sensors are equipped with feedback internal coil.

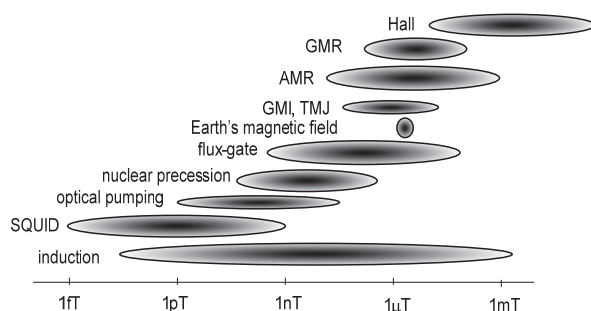


Fig. 1. Typical area of applications of the main magnetic field sensors

From time to time are published various review papers on magnetic field sensors [1-4]. When these papers are

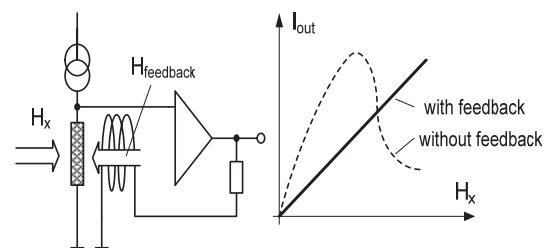


Fig. 2. An example of magnetic field sensor operating with feedback

¹ The paper was presented on ISEF'2013 Conference and is based on the book “Handbook of magnetic measurements” where readers can find much more details.

The lower border of the range (resolution) is limited mainly by noises and zero drift (in the case of DC magnetic fields). Fig. 3 presents typical noise spectrum comparison of two main magnetic field sensors.

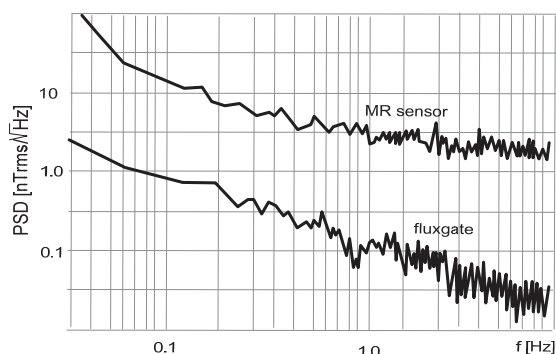


Fig. 3. Typical power spectral density PSD of noise of AMR and fluxgate sensors [5]

From comparison of noise characteristics of two main sensors presented in Fig. 3 we could conclude that generally better is fluxgate sensor because it enables to detect much wider range of magnetic field. But it would be not reasonable to use much expensive fluxgate sensor for the range of magnetic field where more cheaper MR sensor can be used. Similarly not reasonable would be to use very sensitive SQUID sensors in the range where cheaper fluxgate sensor could be used. Figure 4 presents comparison of lower limit of several main sensor (this limit is inversely proportional to sensor cost – the cheapest are AMR sensors, the most expensive are SQUIDs).

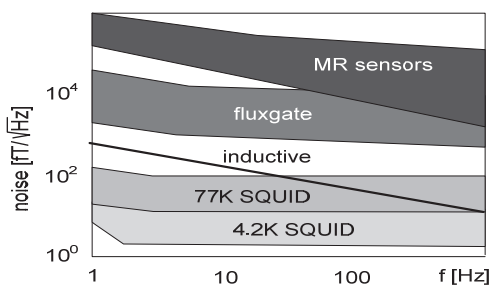


Fig. 4. Comparison of resolution of several main magnetic field sensors

Of course we are able to improve the resolution by using appropriate technique. For suppression of noises the most effective is to use lock-in amplifiers (selective amplification of only carrier frequency signals). Especially easy is for example to use this technique in fluxgate sensors or DC SQUIDs because output signal has well defined carrier frequency (Fig. 5a).

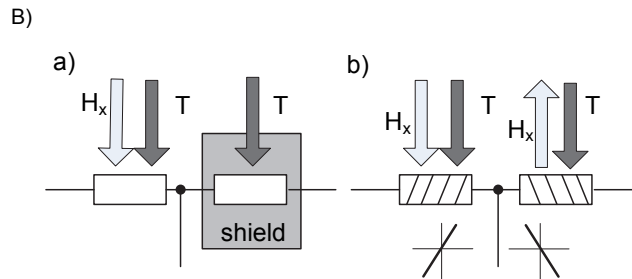
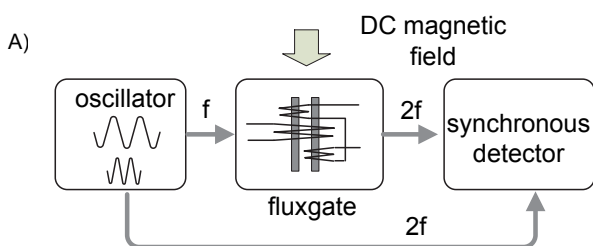


Fig. 5. Main techniques used for improve resolution: A) lock-in amplifier in fluxgate sensor, B) Common mode rejection in GMR (a) and AMR (b) sensors

For decrease of the zero drift, especially temperature zero drift, useful is differential principle illustrated in Fig. 5B. We can detect difference of signals of two sensors: active one (influenced by magnetic field H_x and temperature T) and passive second (influenced only by temperature). The best case is if we can design differential sensors as is in the case of AMR sensors (Fig 5B – right side).

Induction sensors

This sensor [6,7] is usually in form of a coil (with or without ferromagnetic core) and according to the Faraday's law the generated voltage V is proportional to the rate of change of magnetic field

$$(1) \quad V = -n \frac{d\Phi}{dt} = -nA \frac{dB}{dt} = \mu_0 nA \frac{dH}{dt}$$

where: Φ is a magnetic flux, B is flux density, H is magnetic field strength, A is area of the coil, n is number of turns and $\mu_0 = 4\pi \cdot 10^{-7} \text{ Wb/Am}$ is a permeability of the free space.

If magnetic field is varying as sinusoid $B = B_m \sin \omega t$ the induced voltage is

$$(2) \quad V_m = -2\pi n A f B_m$$

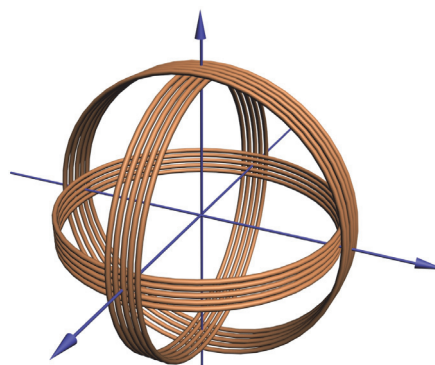


Fig. 6. An example of three-axis coil sensor

Figure 1 demonstrates that induction sensor is the most versatile, enabling measurement of very small magnetic fields (air coil can exhibit sensitivity of 0.3 pT/√Hz at 20 Hz while coils with ferromagnetic core 2.5 pT/√Hz at 1 Hz) [5] as well it can measure large magnetic fields. But this feature is with some limitations or obstacles:

- To obtain high sensitivity the sensor should be rather large because sensitivity depends on coil dimensions. In the case of air coil the diameter of the coil should be as large as possible. Thus for geophysical applications we can meet sensor with diameter larger than one meter and the weight

of hundreds of kilograms. In the case of core sensor the core should as long as possible – thus we can meet sensors for space investigations with length close to one meter.

- Sensor detects only varying magnetic field thus it is not possible to measure DC magnetic fields. But this problem can be solved by design of a moving coil – rotating or vibrating. Moreover large coil enables detection of magnetic fields with very small frequency – even 0.01 Hz thus it is possible to measure quasi-stationary magnetic fields.

- Because output signal depends on derivative of magnetic field it is necessary to use integrating amplifier in the output what can introduce additional errors.

- Output signal depends on frequency of magnetic field. Moreover frequency bandwidth is limited by resonance of the coil. These problems can be solved by using appropriate electronic circuit.

But induction sensor exhibits also several important advantages:

- It is very simply in design. Practically every investigator can easy prepare the sensor by winding a coil.

- In the case of air coil accuracy of the sensor can be very large because according to Eq. (1) output signal depends only on area of the coil, which we can determine with high accuracy.

- We can easy detect all three components of vector of magnetic field using three coils as it is presented in Fig. 6. Therefore such sensor is commonly used to detect electromagnetic pollution.

- The measurement is non-invasive, especially in the case of air coil when neither the ferromagnetic parts nor sensor current disturb measured magnetic field.

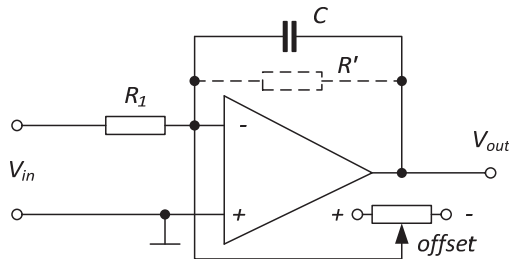


Fig. 7. Typical output circuit of induction coil sensor

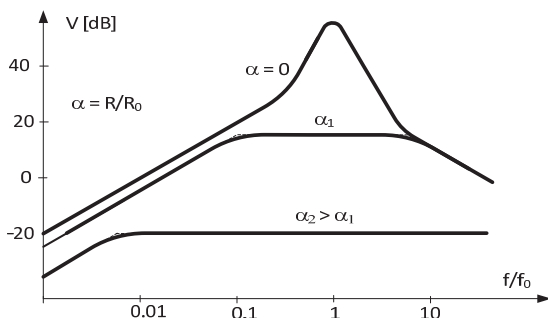


Fig. 8. Frequency characteristic of induction sensor with coil resistance R and load resistance R₀

Fig. 7 presents typical output circuit of induction sensor. Because output signal is proportional to derivative of flux density dB/dt it is necessary to use integrating amplifier. Resistance R_1 should be sufficiently large to avoid load of the coil – typical values are $R_1 = 10 \text{ k}\Omega$, $C = 10 \text{ }\mu\text{F}$.

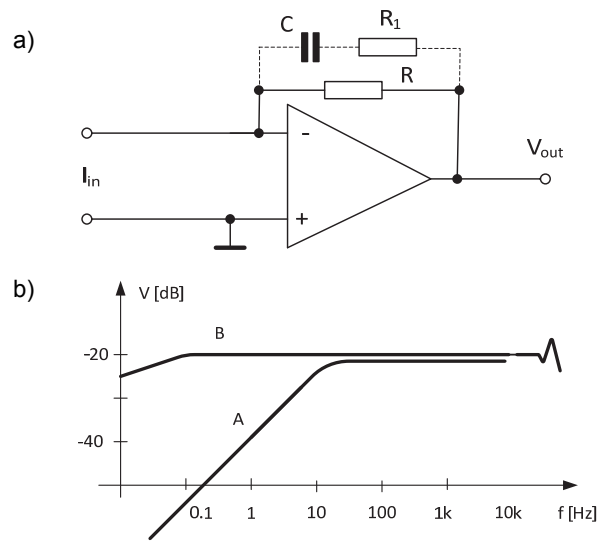


Fig. 9. Current-to-voltage transducer (a) and example of frequency characteristic of the sensor working in current mode (b) (after [8])

It is also possible to use other output circuit – known as self-integrating one. Fig. 8 presents frequency characteristic of the induction sensor. If the sensor is no loaded ($\alpha = 0$) the output signal increased up to resonance frequency f_0 . But if we load the sensor with small resistance the plateau of the characteristics is as wider as smaller load resistance. Thus we can use as an output circuit current-to-voltage transducer presented in Figure 9a. This way we receive transfer characteristic similar to curve A on Fig. 9b. We can additionally improve this characteristic by including correction circuit R_1C (curve B)).

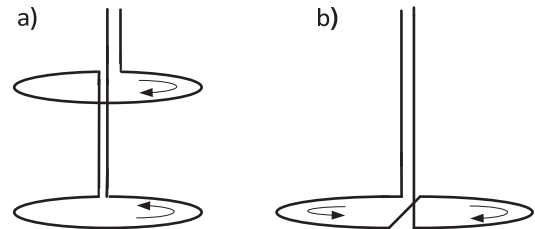


Fig. 10. Gradiometer coils arranged vertically (a) or horizontally (b)

If we measure small magnetic field very convenient is to use gradiometer sensors presented in Figure 10. If we have large magnetic field with source distanced from the sensor and small magnetic field from the local source in both coils common large field is practically the same while field from local source is other in both coils (depending on distance to source). This way we can realize common-mode-rejection.

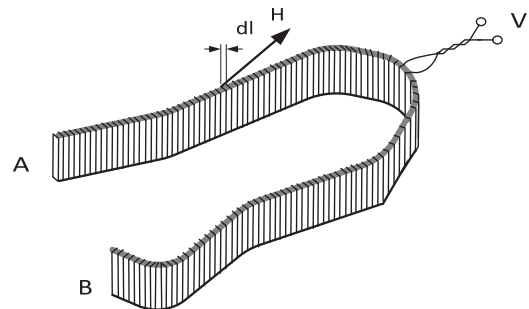


Fig. 11. Rogowski coil sensor

Induction coil sensor (known also as search coil sensor) is commonly used to measure the flux density B . The special design of induction sensor known as Rogowski coil enable to measure the magnetic field strength H . If we wound very regularly turns on the flexible strip (Fig. 11) the induced voltage is the sum of voltages induced in each turn thus it is

$$(3) \quad V = \sum \left(-n \frac{d}{dl} \frac{d\Phi}{dt} \right) = \mu_0 \frac{n}{l} A \frac{d}{dt} \int_A^B H dl \cos \alpha = \mu_0 \frac{n}{l} A \frac{d}{dt} H_{AB}$$

Thus the sensor measures magnetic field strength between point A-B (ends of the coil). This feature is commonly used in magnetic material testing to determine magnetic field strength in the sample (such sensor is also known as RCP – Chattock Rogowski Potentiometer).

Important application of Rogowski coil is contactless measurement of the current I . If we connect ends of the strip and such ring wraps the current conducting wire the sensor detects only the magnetic field generated by the wire and

$$(4) \quad V = \mu_0 \frac{n}{l} A \frac{dI}{dt}$$

Important feature of such sensor is that due to relative small inductance and lack of ferromagnetic parts it can detect very high frequency currents – pulses with time of several nanoseconds.

Fluxgate sensors

The principle of operation of fluxgate sensor is as follows: if we magnetize ferromagnetic core to saturation the induced voltage (in the second coil) is distorted. But because magnetizing curve is symmetrical for both directions of magnetizing field both halves of induced voltage signal are identical. Thus in induced voltage exist only odd harmonics (signal A in Figure 12).

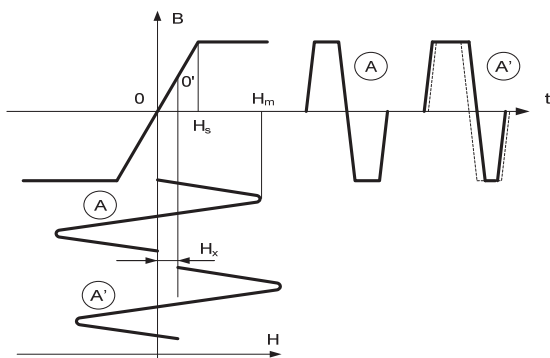


Fig. 12. Principle of operation of fluxgate sensor

If the additional magnetic field H_x appears the operating point on magnetizing curve is shifted (from point 0 to point O') and both halves of induced voltage are different. It results that in this voltage are also even harmonics. Usually as a measure of magnetic field is used the second harmonic in distorted output signal.

Instead of one core two magnetized cores are used with secondary voltages connected reversely (Fig. 13a) – in this way odd harmonics are compensated and in the output exist only even harmonics:

$$(5) \quad e_2 = e_2' - e_2'' = 16n_2 f A \mu H_x \sin \pi \frac{H_s}{H_m} \sin 2\omega t + \dots$$

where: n_2 – number of turns of secondary winding, f – frequency of magnetizing field, A – cross section of the core, μ – permeability of the core.

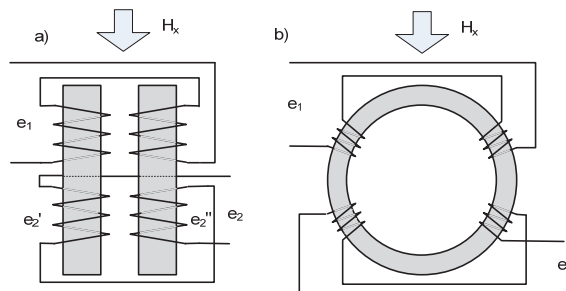


Fig. 13. Two main designs of fluxgate sensor

Usually as the output signal only the second harmonics is used – by applying selective amplifier (or more often synchronous detector with second harmonics of magnetizing signal used as the reference voltage). Assuming typical value of magnetizing field $H_m = 1.5 H_s$ the magnitude of the output signal is

$$(6) \quad E_2 \cong \sim 10n_2 f A \mu_0 \frac{1}{N} H_x = 2n_2 f \mu_0 l^2 H_x$$

where N is demagnetizing factor of the core and l is the length of the magnetized strip.

Thus to obtain high sensitivity the ferromagnetic strips should be as long as possible with large number of secondary turns and high frequency of magnetizing field. For typical values $n_1 = n_2 = 1000$, $f = 3 \text{ kHz}$, $l = 2 \times 60 \text{ mm}$, $A = 3 \times 0.1 \text{ mm}$ it is possible to obtain sensitivity $10 \mu\text{V/nT}$.

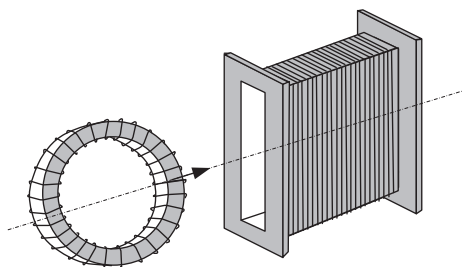


Fig. 14. Typical design of ring core sensor

Recently more often is used sensor in form of a ring (Fig. 13b) where two halves of a ring substitute two strips. Such design is much easy to prepare (see Fig. 14) and what is important it needs much less magnetizing power what can be important in space research [10].

Fluxgate magnetometers have many advantages and therefore are commonly used, especially in military applications and space research. They are relative cheap and easy to prepare, with high sensitivity (even 10 mV/nT [11]) with resolution of about 10 pT . Because output signal as an AC signal problem of zero drift is easy to solve as well problem of noises is decreased due to applying lock-in amplifier (see Fig. 5A).

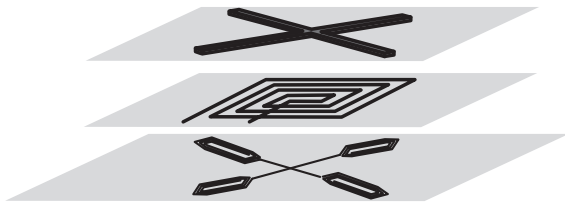


Fig. 15. The example of two-axis miniature sensor prepared by thin film technology [12,13]

Recently fluxgate sensor are often miniaturized by using PCB or thin film technology. Such miniature sensors can be magnetized with much higher frequency and can be prepared as two-axis sensors, often with integrated electronics. Fig. 15 presents example of such design. The sensor with dimensions 2.5×2.5 mm (including electronics) exhibited sensitivity of $3.8 \text{ mV}/\mu\text{T}$ for 125 kHz excitation.

Magneto resistive sensors

There are many various magneto resistive effects [14] (see Fig. 16) but recently only three main effects are commonly used – AMR effect, spin valve effect and magnetic tunnel junction MTJ.

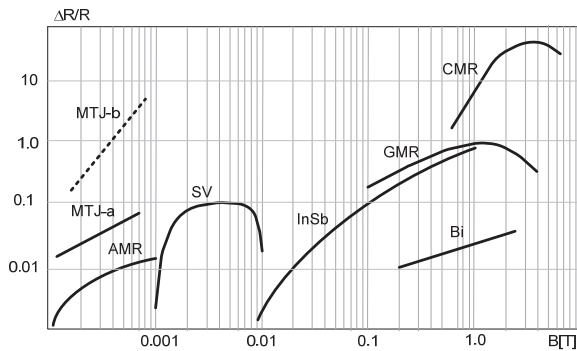


Fig. 16. Various magneto resistive effects: AMR – anisotropic magnetoresistance, GMR – giant magnetoresistance, SV – spin valve sensor, MTJa – magnetic tunnel junction with Al-O spacer, MTJb – magnetic tunnel junction with Mg-O spacer, InSb – semiconductor sensor, CMR – colossal magnetoresistance, Bi – bismuth [1,14]

AMR sensors

AMR sensors are treated as slightly old-fashioned sensors (the effect was discovered in 1857 by Kelvin and sensors are mainly developed in 1970-1980). These sensors are shadowed by new GMR sensors but they still have many interesting advantages:

- they are very simple in preparation, thus cheap market available sensors are still available;
- they have better sensitivity than GMR sensors, typical sensor of Philips KMZ10B has sensitivity $20 \mu\text{V}/(\text{A}/\text{m})$ (about $16 \mu\text{V}/\mu\text{T}$) – GMR sensors of NVE have similar sensitivity but with flux concentrators);
- it is easy to prepare differential pairs of sensors and by using such sensors it is possible to remove influence of temperature (in the case of GMR sensors the same result is possible to obtain by using pair passive/active sensors – see Fig. 5B).

The main disadvantages of AMR sensors are as follows:

- relative small change of resistance, not exceeding 2 %;
- sensitivity to orthogonal component – this component H_y should not exceeding $0.1 H_x$;

- possibility of demagnetization by high magnetic field. This effect can be reversed by again magnetizing of a sensor.

AMR effect is very simple – resistance of an anisotropic ferromagnetic material depends on direction of magnetization. Although this effect is known for a long time the development of the sensors was possible after introduction of thin film technology, because in thin ferromagnetic films relation between external magnetic field and direction of magnetization is explicitly determined. The angle φ of magnetization (related to anisotropy axis of material with anisotropy field H_k) is

$$(7) \quad \sin \varphi = \frac{H_x}{H_k + H_y}$$

On the other hand the change of resistance is

$$(8) \quad \frac{\Delta R_x}{R_x} = -\frac{\Delta \rho}{\rho} \sin^2 \vartheta$$

where $\Delta \rho/\rho$ is a magneto resistivity coefficient and ϑ is an angle between direction of magnetization and direction of a current. Thus for a strip directed along an anisotropy axis $\vartheta = \varphi$ and we obtain relation

$$(9) \quad \frac{\Delta R_x}{R_x} = -\frac{\Delta \rho}{\rho} \frac{H_x^2}{(H_k + H_y)^2}$$

This relation is nonlinear. The simple method of linearization is to direct the current with the angle $\pm 45^\circ$ with respect to anisotropy axis. This way $\vartheta = 45 - \varphi$ and for $H_x \ll H_k$ we obtain

$$(10) \quad \frac{\Delta R_x}{R_x} \cong \frac{\Delta \rho}{\rho} \left(\frac{1}{2} \pm \frac{H_x}{H_k + H_x} \right)$$

Thus we obtain almost linear sensor and sensor with angle 45° is differential with respect to the sensor of -45° – see Fig. 17.

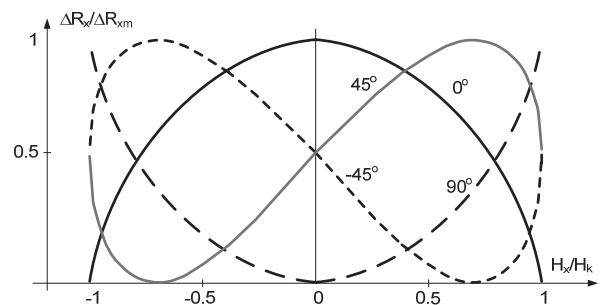


Fig. 17. Transfer characteristics of the AMR sensors with current direction along anisotropy axis 0° and inclined by $\pm 45^\circ$

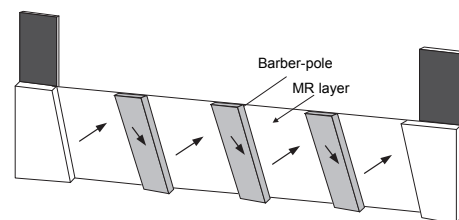


Fig. 18. Transfer characteristics of the AMR sensors with current direction along anisotropy axis 0° and inclined by $\pm 45^\circ$

The most popular method of inclination of the direction of current by 45° to anisotropy axis is a design proposed by Kuijk known as a Barber-pole sensor [15,16]. By deposition of additional electrodes from good-conducting material we force the direction of current as it is presented in Fig. 18. Usually the AMR sensor is composed of two pairs of differential sensors connected into bridge circuit. This way the sensor converts directly magnetic field into output voltage. The example of the design of AMR sensor KMZ10B and its transfer characteristic are presented in Fig. 19. Often such sensor is equipped with two additional planar coils – one to realize the feedback, the second to magnetize the sensor. Similar design and parameters have sensors of Honeywell – for example sensor HMC1001 with sensitivity 200 $\mu\text{V}/(\text{A/m})$. Such sensors are used as electronic compasses.

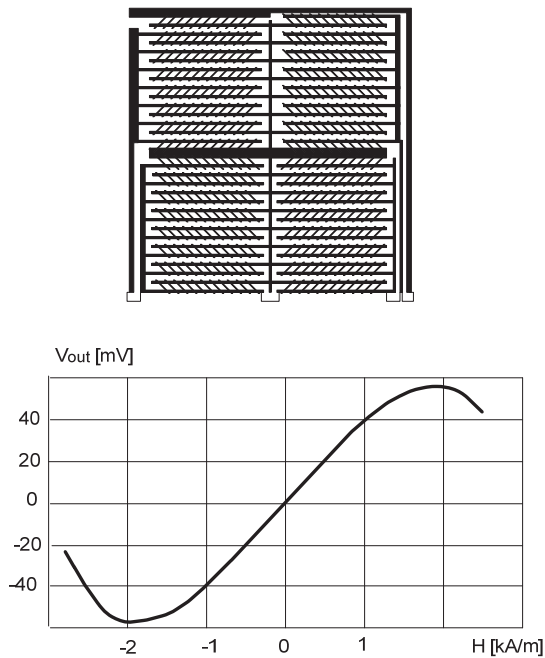


Fig. 19. The design and transfer characteristic of KMZ10B AMR sensor

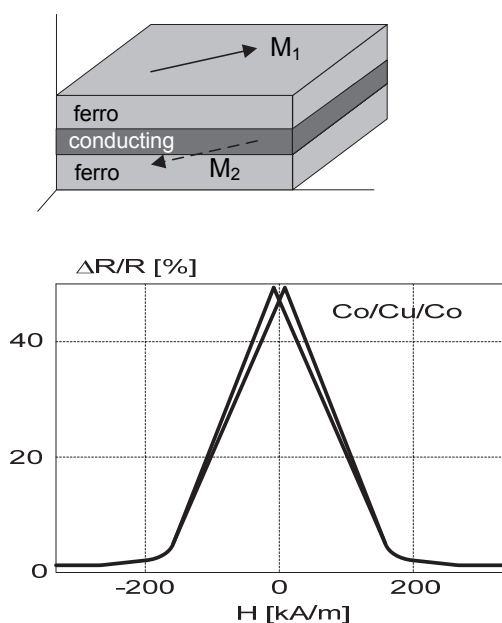


Fig. 20. The design and transfer characteristic of GMR sensor [18]

GMR and spin valve sensors

The GMR sensors discovered by team of A. Fert (and honored by Nobel prize) [17] use another magnetoresistive effect – in two thin ferromagnetic films separated by third very thin film from conducting material (spacer) transition from initial antiparallel state of magnetization (two films of opposite directions of magnetization) to parallel state (the same directions of magnetization) is accompanying by very large (even larger than 100%) change of resistance (Fig. 20).

This original GMR device is recently substituted by other design proposed by Dieny and co-workers and known as spin valve sensor [19]. The main drawback of classical GMR effect was pure sensitivity. Antiparallel state was obtained by strong coupling of two layers separated by very thin spacer. To overcome this coupling high external magnetic field is necessary. In spin valve sensors the antiparallel magnetization is obtained artificially – by deposition of additional layer of antiferromagnetic material. In this way one ferromagnetic film (pinned) is magnetized in another way than the second one (free layer).

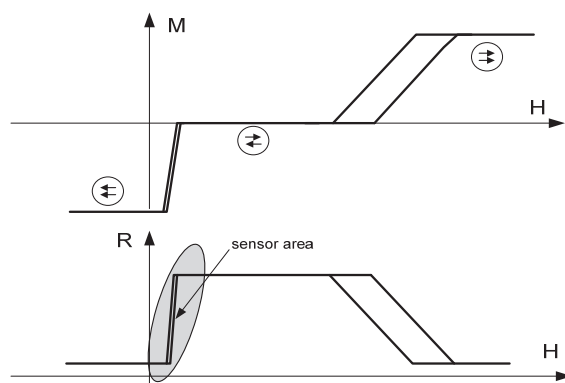


Fig. 21. The principle of operation of spin valve sensor

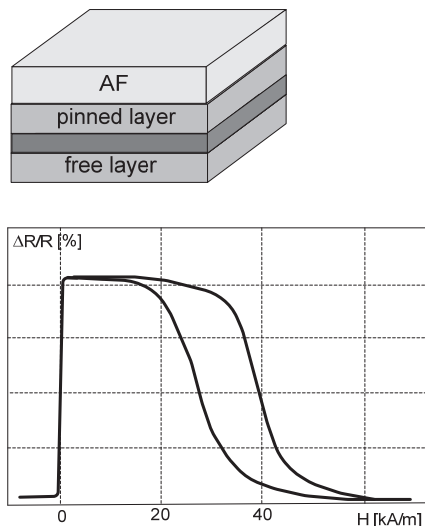


Fig. 22. The design and transfer characteristic of spin valve sensor [20]

Fig. 21 illustrates principle of operation of a spin-valve sensor. Initially (for $H_x = 0$) both layers are magnetized parallel. When external magnetic field increases as first change the direction of magnetization free layer. Thus we have transition from parallel to antiparallel state and accompanying change of resistance. After further

increasing of magnetic field also second pinned layer changes direction of magnetization and we return to parallel state (with accompanying change of resistance). In the spin valve sensor the distance between layers can be larger because a strong coupling is not necessary to obtain antiparallel order. This way we obtain larger sensitivity (see Fig. 16) but at the cost of change of resistance – it not exceeds 25% (although it is tenfold larger in comparison with AMR effect). Fig. 22 presents design and typical transfer characteristic of spin-valve sensor.

Magnetic tunnel junction sensors

These sensors are similar to spin valve sensors with one difference – instead of conducting spacer it is used thin insulating layer.

Initially the spacer was prepared from oxidized aluminum. Such sensors have quite large magneto-resistance (about 40%) for relative small magnetic field – see MTJ-a on Fig. 16. But problems with noises and small polarization voltage caused that progress was not significant – see Fig. 23.

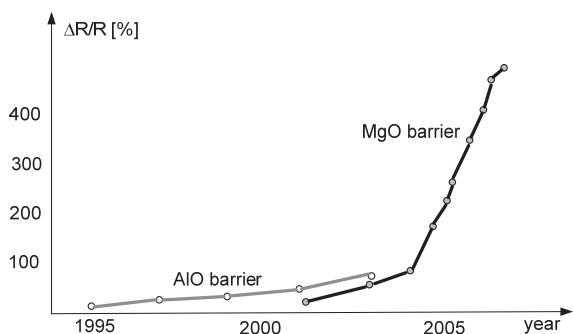


Fig. 23. Progress in performances of magnetic tunnel junction sensors [21]

The turning point appeared in 2004 when Parkin and Yuasa [22,23] proved that by applying barrier from crystalline textured MgO it is possible to obtain significant increase of magnetoresistance of MTJ sensors. Indeed they reported magnetoresistance as large as 180 and 220%. Soon after this disclosure development of MTJ sensors resulted in receiving of the magnetoresistance larger than 500% (Fig.24). Recently the magnetic tunnel junction is the best candidate to design magnetic memory elements.

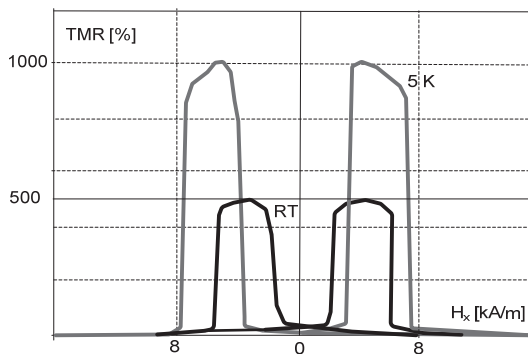


Fig. 24. Magnetic MgO tunnel junction with tunnel magnetoresistance TMR close to 1000% [24]

Hall effect sensors

Hall sensors [25] discovered in 1879 are still one of the most often used magnetic field sensors. They have many advantages and one quite important drawback – not too high sensitivity, not exceeding 5 mV/mT.

The advantages are as follows:

- simple design and technology of manufacturing. Thus sensors can be very cheap although sensors for magnetic field measurement with high linearity and small temperature errors are expensive.
- possibility to design very small sensors, with dimensions of several μm (and even smaller than $1 \mu\text{m}$ [26]).
- noninvasive measurement of magnetic field – lack of ferromagnetic elements, although supplying current can generate small magnetic field.

The principle of operation is illustrated in Fig. 25. Without magnetic field current lines are regular and on the electrodes does not exist output voltage V_H . External magnetic field introduces asymmetry due to Lorentz force and output voltage V_H is proportional to magnetic field B .

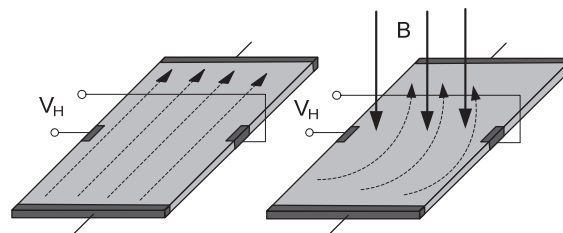


Fig. 25. Current lines in Hall device without and with presence of magnetic field B

The output voltage depends on the carrier mobility μ . For the sensor with length l , width w the output voltage is

$$(11) \quad V_H = \mu \frac{w}{l} V_0 B_x$$

The most important parameter is carrier mobility μ and it depends on material of Hall device. For the most popular materials it is: InSb – 80 000, InAs – 33 000, GaAs – 8 500, Si – 1 400 cm^2/Vs . The largest parameter μ exhibits indium antimonide but such sensors have rather large temperature errors. Therefore on the market are available sensors prepared from other materials with typical sensitivity – InAs or GaAs sensors with sensitivity of about 0.2 mV/mT (sensors of F.W.Bell/Sypris) or InSb – 5 mV/mT (sensors of Asashi Kasei).

Although silicon has rather small carrier mobility it is commonly used for IC Hall sensors because it is easy to integrate with silicon electronics. Recently IC Hall sensors with amplifier and temperature errors correction are dominating on the market. For example integrated Hall sensor HAL 401 of Micronas with dimensions $0.37 \times 0.17 \text{ mm}$ exhibits sensitivity of about 50 mV/mT, range $\pm 50 \text{ mT}$, nonlinearity error less than 0.5% for FS and frequency bandwidth 0 – 10 kHz.

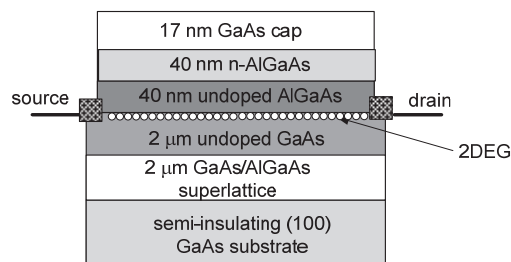


Fig. 26. The heterostructure of micro-Hall 2DEG sensor [27]

Recently to prepare very small micro-Hall sensors new technology is used, known as 2DEG (2D electron gas) or quantum well. In this structure the semiconductor film is very thin (several nm) and this way carrier can be transferred only in that plane (high 2D mobility). Fig. 26 presents sensor with dimensions 0.8x0.8 mm used to scanning Hall microscopy.

Typical Hall sensors detect magnetic field perpendicular to sensor plane (see Fig. 25) but in special design is possible to prepare vertical sensor as well three-axis sensors [28].

SQUID sensors and magnetometers

The highest sensitivity exhibit SQUID sensors – with noises of about $5\text{fT}/\sqrt{\text{Hz}}$ they enable to detect fT magnetic field (in typical application pT). Therefore they are commonly used to analyze of magnetic field resulting from brain activity. Recently also NDT techniques profit this high sensitivity to detects and even to forecast defects [29].

The most commonly used DC SQUID is in form of a thin film ring with two symmetrical tunnel junctions (Josephson junctions) not larger than 0.1 – 0.2 nm (RF SQUID requires only one tunnel junction). Usually this device is prepared from niobium that has relative large critical temperature 9.3 K enabling to use for a cooling a liquid helium (it is also possible to use “high” temperature ceramic materials with critical temperature of about 120 K but such sensors are more noisy).

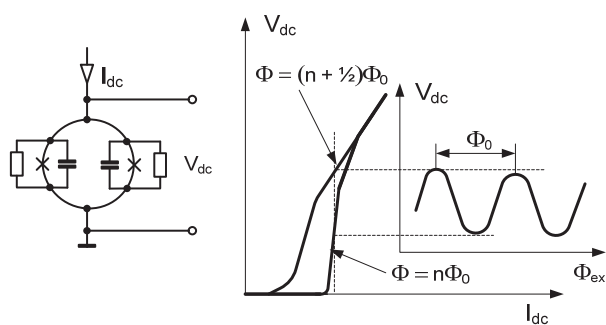


Fig. 27. The principle of operation of DC SQUID [30]

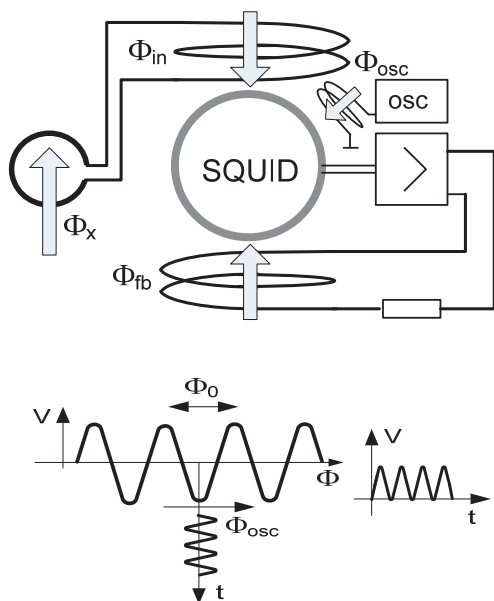


Fig. 28. DC SQUID magnetometer with feedback and second harmonic detection

Fig. 27 presents principle of operation of DC SQUID. In this device supplied by DC current due to quantization of magnetic flux output voltage versus external magnetic flux is in form of sinusoid with a period equal to

$$(12) \quad \Phi_0 = \frac{h}{2e} = 2.067833667 \times 10^{-15} \text{ Wb}$$

If we assume that a ring has a cross section of about 1 cm^2 (in practice it can be much smaller) this corresponds with flux density $2.067 \times 10^{-11} \text{ T}$.

Usually only small parts of $V_{\text{DC}} = f(\Phi_{\text{ex}})$ characteristic is used because sensor operates as zero field detection due to feedback. To decrease noises and zero drifts often additional magnetizing coil and oscillator are used – this way we can use AC lock-in amplifier tuned to second harmonics. Often the same coil serves as a feedback and modulation.

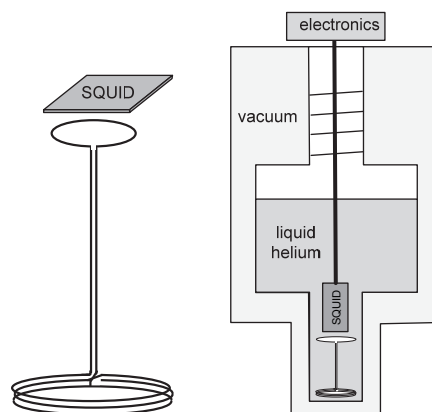


Fig. 29. The flux transformer and the Dewar flask used in SQUID magnetometers

It is not necessary to insert directly SQUID device in measured magnetic field. Often this field is detected by flux transformer with gradiometer coil as it is presented in Fig. 29. Therefore such detecting coil can be very small what enables to design SQUID microscope as it is presented in Fig. 30.

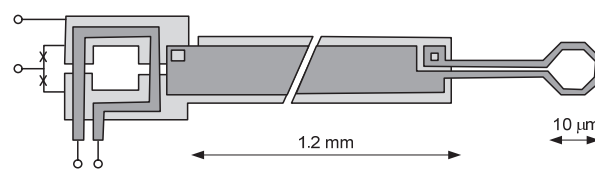


Fig. 30. The micro-SQUID sensor for microscopy application [31]

Resonance sensors and magnetometers

Resonance magnetometers have many unique features. Electron resonance sensors (optically pumped sensors) have very high sensitivity close to SQUID sensors – therefore they are used in space research and for detection of metal parts from large distance. All resonance methods have extremely large accuracy because we know the gyromagnetic factor very exactly. Thus NMR magnetometers can be used to calibrate Hall magnetometers.

They have also some drawbacks. Usually sensors are rather large (especially in free precession magnetometer), consumes much power (especially in optically pumped sensors). They usually measures scalar magnetic fields although in special cases also possible is vector

measurement. Most of these magnetometers do not measure magnetic field continuously. Magnetic field should be uniform and generally we measure only constant magnetic fields. And with exception of free precession magnetometers they are rather expensive what limit their application to special purposes – mainly geophysics and military applications (for example detection of metal objects).

Protons or electrons are rotating due to spin. Because they have electric charge this rotation results in magnetic moment. If we put such rotating part into external magnetic field the torque causes that particles act as a gyroscope rotating with precession around the direction of external field. For constant magnetic field the frequency of this rotation depends only on gyromagnetic factor γ and value of magnetic field B

$$(13) \quad \omega_0 = \gamma B$$

We know very exactly the value of gyromagnetic factor equal to

$$\gamma_p = 42.576375 \text{ MHz/T}$$

for protons and

$$\gamma_e = 28.1481 \text{ GHz/T}$$

for electrons.

Free precession nuclear magnetic resonance NMR magnetometers

The principle of operation of such magnetometers is presented in Fig. 31. In the first step we polarize cell with proton rich substance (for example water or benzene) with constant large magnetic field generated by coil wound on the cell. In the second step we disconnect polarizing field and connect the same coil to amplifier. We observe decaying oscillations where frequency of oscillation is proportional to measured magnetic field according to Eq. (13).

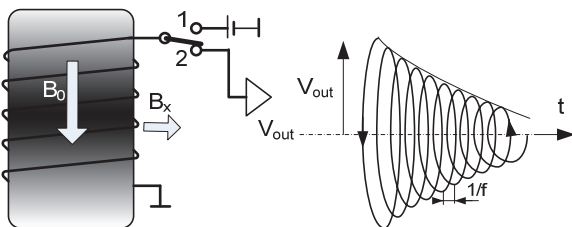


Fig. 31. The principle of operation of proton free precession sensor

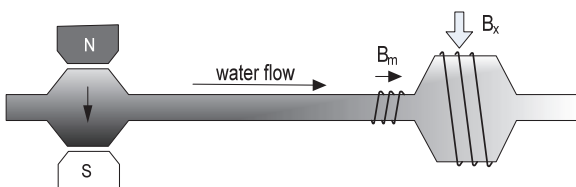


Fig. 32. Sensor with flowing water

The principle of operation of such magnetometer seems to be very simple. But to correct design some problems should be solved. Output oscillating signal is usually very small with noises and fast decaying. The fast disconnection of the same coil of high inductance may cause overvoltage. Due to small value of gyromagnetic factor measured

frequency is not very large – Earth's magnetic field $50 \mu\text{T}$ corresponds with frequency of only 2130 Hz. Market available free precession proton magnetometers – model G-856 of Geometrics has resolution 0.1 nT, range 20 – 90 μT , sensor dimensions $9 \times 13 \text{ cm}$.

Important drawback of sensor presented in Fig. 31 is discontinuity of measurements – one cycle needs several seconds. This problem can be solved in sensor with flowing water presented in Fig. 32. It is composed of two cells – one for polarization (by magnet or additional coil), the second is used to measure the precession frequency.

Nuclear magnetic resonance NMR magnetometers

Such magnetometers are used for very accurate measurement of large magnetic fields. The market available magnetometer PT2026 of Metrolab enables measurement of magnetic field in range 0.2 – 20 T with accuracy 5 ppm and resolution 0.01 ppm. The principle of operation is presented in Fig. 33.

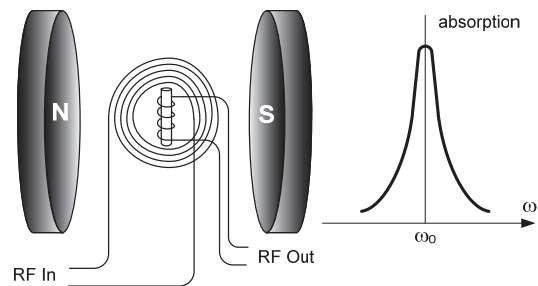


Fig. 33. The principle of operation of NMR magnetometer

The magnetic field used to calibration of other devices can be generated by permanent magnet. To detect resonance conditions two additional coils are used – one to tune the sensor with RF magnetic field (perpendicular to measured magnetic field), the second one to detection of resonance (wound on the cell). RF frequency is changed and for resonance frequency the delivered energy is absorbed in the most efficient way.

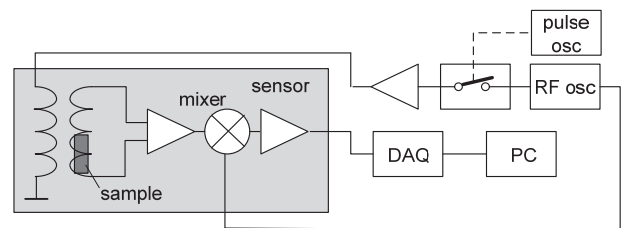


Fig. 34. Integrated NMR sensor [32]

Fig. 34 presents integrated sensor of NMR resonance. It consists of two planar coils and amplifier. Solid sample has volume only 1 mm^3 . The exciting coil is supplied by $40 \mu\text{s}$ pulses from external oscillator. The output signal is analyzed with the Fourier transform by external computer.

Optically pumped electron spin resonance ESR sensors

Electron spin resonance has much larger gyromagnetic factor than NMR and therefore it enables measure much smaller magnetic fields. Market available potassium magnetometer of GEM Systems has resolution 0.1 fT, range 20 – 100 μT and accuracy 0.1 nT.

In the ESR optical magnetometers to detect external magnetic field the Zeeman effect is used. Under the influence of external magnetic field the energy spectral

levels are split into several sublevels as it is presented in Fig. 35. Thus transition between levels and emission or absorption of light depends on magnetic field. Absorption of this light is the largest for resonance frequency.

Fig. 36 presents an example of the helium ^4He optical pumping magnetometer. The cell filled by helium is illuminated by polarized light of length 1083 nm corresponding with transition between 2^3S_1 and 2^3P_0 energy levels. The polarized light serves to excite the cell substance similarly as large magnetic field in NMR resonance (optical pumping principle).

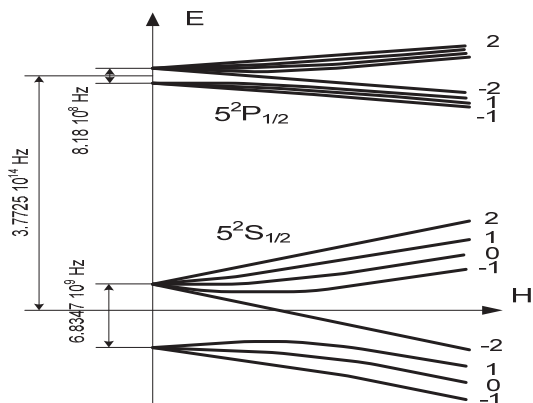


Fig. 35. Splitting of the energy levels of rubidium Rb87 versus magnetic field H – Zeeman effect

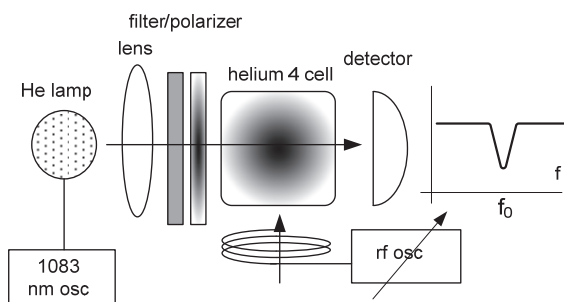


Fig. 36. An example of the optically pumped magnetometer

In the fully optically pumped state the transparency of the cell is the best – light intensity is the largest. Now if we use additional RF coil the light intensity (opacity of the cell) depends on the frequency of this field. For resonance condition the light intensity is the smallest.

Various substances can be used as an optically pumped cell. The most often used are: cesium with gyromagnetic factor $\gamma = 3.498 \text{ Hz/nT}$ and resonance curve width $\Delta\omega = 20 \text{ nT}$; potassium with $\gamma = 7.005 \text{ Hz/nT}$ and $\Delta\omega = 1 \text{ nT}$ and helium with $\gamma = 28.025 \text{ Hz/nT}$ and $\Delta\omega = 70 \text{ nT}$. Helium exhibits the largest γ factor but the best resolution has potassium due to narrow resonance curve. Cesium and potassium required additional heating to obtain vapor while helium is gaseous so heating is not necessary.

Overhauser magnetometer sensors

Optically pumped magnetometers have very high sensitivity but the require power for light and heating and the whole device is usually complex and expensive. As alternative can be considered the Overhauser magnetometer.

In the Overhauser magnetometer (known also as dynamic nuclear polarization DNP magnetometer) the cell is

filled with mixture of proton rich substance (for example methanol) and free electron rich substance – usually nitroxide free radical. This way both resonances NMR and ESR can exist in one cell and ESR resonance can be used to polarize NMR cell (instead of large magnetic field).

Overhauser magnetometer joints advantages of both NMR and ESR methods – simplicity, low power consumption, high sensitivity and additionally almost continuous operation. Indeed market available Overhauser magnetometer GSM-19 of GEM Systems has resolution 10 fT, accuracy 0.1 nT and speed 5 samples/s.

Other sensors and principles

Giant magnetoimpedance sensors

The giant magnetoimpedance GMI sensors are in form of microwire, thin film or thin ribbon (most often wire) supplied by high frequency current. Two effects cause change of impedance – dependence of permeability on external constant field and skin effect. Due to these effects change of impedance can be very large (even 400%) for relative small magnetic field, below 1 kA/m. Fig. 37 presents transfer characteristic of the GMI sensor connected in the Colpitts oscillator.

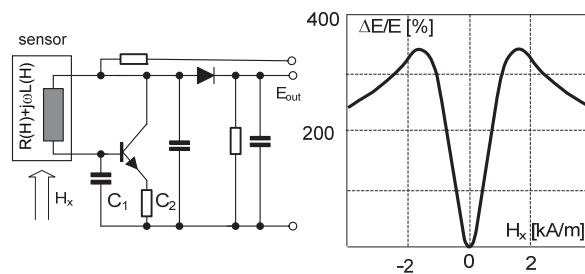


Fig. 37. GMI sensor connected in the Colpitts oscillator [33]

In 2001 Aichi Microintelligent Corporation started with manufacturing of various transducers (magnetic field sensor, compass) based on GMI sensor. As the sensor is used an amorphous wire with diameter $20 \mu\text{m}$ and length 2 mm on which are wound two coils – for bias and feedback – Fig. 38.

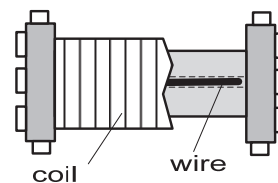


Fig. 38. GMI sensor of Aichi Microintelligent Corporation [34]

This sensor is fed by pulse oscillator and sensitivity of $1\text{V}/\mu\text{T}$ is reported. The digital magnetic field meter basing on this sensor MGM-1DS measures magnetic field in the range of $200 \mu\text{T}$ with resolution 10 nT.

Extraordinary magnetoresistance

In 2000 Solin and co-workers published information about extremely large magnetoresistive effect (even million percent) in special heterostructure consisting of semiconductor and metal shunt [35]. In contrary to other magnetoresistors this effect results not from material properties but it is obtained by applying of the special geometrical conditions.

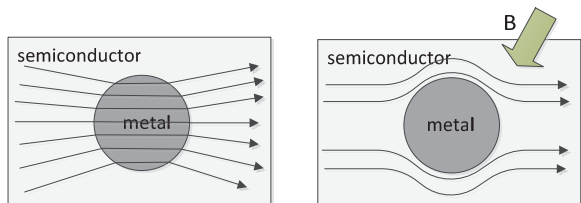


Fig. 39. Principle of operation of EMR sensor [36]

Fig. 39 presents the principle of operation of EMR sensor. In absence of external magnetic field lines of current are regular. In presence of magnetic field current lines are changed due to Lorentz force (see also Fig. 25) and avoid metal shunt. This way resistance of the sensor changes extraordinary.

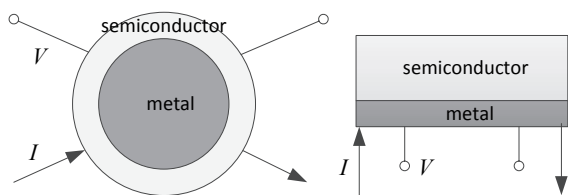


Fig. 40. Two examples of EMR sensors

This effect strongly depends on geometry as well on carrier mobility of semiconductor and conductivity of metal part. Various shapes of the sensor have been proposed – see Fig. 40.

Sensitivity of typical EMR sensors is rather small – they require magnetic field of several Tesla. In application as reading head it is not a significant drawback because generally magnetic field of the disk is large. But so far there are no reports about practical applications of these sensors.

Magneto-optical sensors

In the fiber optic sensor presented in Fig. 41 the laser beam is transmitted by two glass fibers – the reference one and the second connected to magnetostrictive elements. In presence of magnetic field the second line changes the length. Although this change is rather small the interferometer enables to detect such changes with exceptionally resolution. Thus it is reported that such sensor detects magnetic field with resolution of pT at room temperature. It can be used to detect undersea ships traffic [37,38].

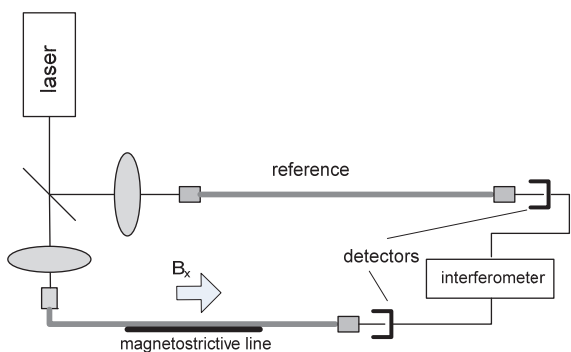


Fig. 41. Fiber optic magnetic field sensor

Another magneto-optical sensor applying Faraday effect is presented in Fig. 42. Polarized light is transmitted via fiber wire to an active part, usually garnet crystal. According to Faraday effect this light changes the angle of polarization and value of this angle β depends on value of magnetic field

$$(14) \quad \beta = \nu l B$$

where ν is a Verdet constant and l is the length of the crystal.

The Wollstone prism enables to detect angle of rotation of the polarized light. Such sensors are used as contactless current sensors in high voltage lines.

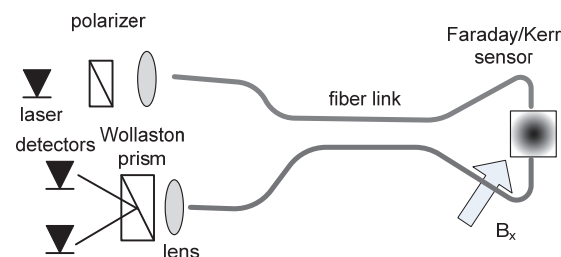


Fig. 42. Magneto-optical sensor applying Faraday effect

MEMS sensors

Fig. 43 presents two examples of magnetic field sensors prepared by using a micromechanical technology MEMS. The first sensor resembles a classical magnetic needle compass device. The small balance is deflected under influence of magnetic field. This deflection is detected by capacitance method [39].

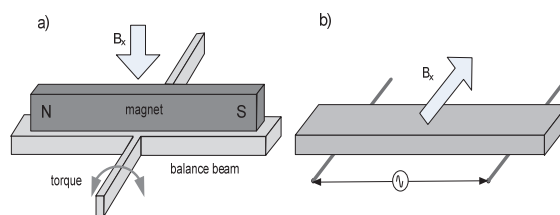


Fig. 43. Two examples of MEMS magnetic field sensors

The second sensor (Fig. 43 b) operates as a xylophone resonator. The aluminum bar is vibrating under influence of AC supplying current. The damping of vibration depends on external magnetic field. Vibrations are detected by laser beam [40].

REFERENCES

1. S. Tumanski – Handbook of magnetic field measurements, Ch.4 – Magnetic sensors, CRC Press 2011
2. S. Tumanski – A review of magnetic sensors, Przegł. Elektr., 80 (2004), 74-80
3. Lenz J., Edelstein A.S. – Magnetic sensors and their applications, IEEE Sensors J., 6 (2006), 631-649
4. Ripka P. (Ed) – Magnetic sensors and magnetometers, Artech House, 2001
5. Ripka P. - Noise and stability of magnetic sensors, J. Magn. Mat., 157-158 (1996), 424-427
6. Tumanski S. – Induction coil sensors – a review, Meas.Sc.Technol., 18 (2007), R31-R47
7. Prance R.J., Clark T.D., Prance H., Room temperature induction magnetometers, in Encyclopedia of Sensors, American Scientific Publishers, 2006
8. Prance R.J., Clark T.D., Prance H. – Ultra low noise induction magnetometer for variable temperature operation, Sens. Act., 85 (2000), 361-364

- 9 Ripka P. – Advances in fluxgate sensors, *Sens. Act.*, A106 (2003), 8-14
- 10 Husmann G., Afanassiev Y. – Fluxgate magnetometers for space research, Books on Demand GmbH, 2010
- 11 Saito T., Fluxgate magnetometer with a 0.5 m length two core sensor, *Sci.Rep. Tohoku Univ.*, 27 (1980), 85-93
- 12 Chiesi L., Keijk P., Janossy B., Popovic R.S. – CMOS planar 2D microfluxgate sensor, *Sens. Act.*, 82 (2000), 174-180
- 13 Drljaca P.M., Keijk P., Vincent F., Piquet D., Gueissaz F., Popovic R.S., - Single core fully integrated CMOS microfluxgate magnetometer, *Sens. Act.*, A110 (2004), 236-241
- 14 Tumanski S. – Thin film magnetoresistive sensors, *IOP Publ.*, 2001
- 15 Kuijk K.E., van Gestel W.J., Gorter F.W. – The Barber pole, a linear magnetoresistive heads, *IEEE Trans. Magn.*, 11 (1975), 1215-1217
- 16 Tumanski S., Stabrowski M. – The optimization and design of magnetoresistive Barber-pole sensors, *Sens.Act.*, 7 (1985), 285-295
- 17 Baibich M.N., Broto J.M., Fert A., van Dau F.N., Petroff F. – Giant magnetoresistance of (001)Fe/(001)Cr magnetic superlattices, *Phys. Rev. Lett.*, 61 (1988), 2472-2475
- 18 Parkin S.S.P., Bhadra R., Roche K.P. – Oscillatory magnetic exchange coupling through thin copper layer, *Phys. Rev. Lett.*, 66 (1991), 2152-2155
- 19 Dieny B., Speriosu V.S., Gurney B.A., Parkin S.S.P., Wilhoit D.R., Roche K.P., Metin S., Peterson D.T., Nadimi S. – Spin-valve effect in soft ferromagnetic sandwiches, *J. Magn. Magn. Mat.*, 93 (1991), 1201-104
- 20 Dieny B., Speriosu V.S., Metin S., Parkin S.S.P., Gurney B.A., Baumgart P., Wilhoit D.R. – Magnetotransport properties of magnetically spin valve structures, *J. Appl. Phys.*, 69 (1991), 4774-4779
- 21 Zhu Jiang-Gang, Park Ch. – Magnetic tunnel junctions, *Materials Today*, 9 (2006), 36-45
- 22 Parkin S.S.P., Kaiser C., Panchula A., Rice P.M., Hughes B., Sumant M., Yang S.H. – Giant tunneling magnetoresistance at room temperature with MgO (100) tunnel barriers, *Nat. Mater.* 3 (2004), 862-867
- 23 Yuasa S., Nagahama T., Fukushima A., Suzuki Y., Ando K. – Giant room temperature magnetoresistance in magnetic tunnel junctions with a crystalline Fe/MgO/Fe magnetic tunnel junctions, *Nat. Mater.*, 3 (2004), 868-871
- 24 Lee Y.M., Hayakawa J., Ikeda S., Matsukura F., Ohno H. – Effect of electrode composition on the tunnel magnetoresistance of pseudo spin valve magnetic tunnel junction with MgO tunnel barrier, *Appl. Phys. Lett.*, 90 (2007), 212507
- 25 Popovic R.S. – Hall effect devices, *IOP publ.*, 2004
- 26 Boero G., de Mierre M., Besse P.A., Popovic R.S. – Micro Hall devices: performance, technologies and applications. *Sens. Act. A106* (2003), 314-320
- 27 Sandhu A., Masuda H., Oral A., Bending S.J.. – Room temperature magnetic imaging of magnetic storage media and garnet epilayers in the presence of external magnetic field using a submicron GaAs SHPM, *J. Cryst. Growth.*, 227-228 (2001), 899-905
- 28 Schott C., Waser J.M., Popovic R.S. – Single chip 3D silicon Hall sensor, *Sens. Act.* 82 (2000), 167-173
- 29 Krause H.J., Kreutzenbruck M. – Recent development in SQUID NDE, *Phys. C* 368 (2002), 70-79
- 30 Clarke J., Braginski A.I. (Ed) – *The SQUID handbook*, Wiley-VCH, 2004
- 31 Kirtley J.R., Wikswo J.P. – Scanning SQUIDS microscopy, *Ann. Rev. Mat.*, 29 (1999), 117-148
- 32 Boero G., Frounchi J., Furrer B., Besse P.A., Popovic R.S. – Fully integrated probe for proton nuclear magnetic resonance magnetometry, *Rev. Sc. Instr.*, 72 (2001), 2764-2768
- 33 Uchiyama T., Mohri K., Panina L.V., Furuno K. – Magnetoimpedance in sputtered amorphous films for micromagnetic sensor, *IEEE Trans. Magn.*, 31 (1995), 3182-3184
- 34 Honkura Y. – Development of amorphous wire MI sensor for automotive use, *J. Magn. Magn. Mat.*, 249 (2002), 375-381
- 35 Solin S.A., Thio T., Hines D.R., Heremans J.J. – Enhanced room temperature geometric magnetoresistance in inhomogeneous narrow-gap semiconductor, *Science* 289 (2000), 1530-1532
- 36 Sun J., Kosel J. – Extraordinary magnetoresistance in semiconductor/metal hybrids: a review, *Materials*, 6 (2013), 500-516
- 37 Bucholtz F at al. – Demonstration of a fiber optic array for three axis magnetometers for undersea applications, *IEEE Trans. Magn.*, 31 (1995), 3194-3196
- 38 Sedlar M., Matejec V., Paulicka I. – Optical fibre magnetic field sensor with ceramic magnetostrictive jacket, *Sens. Act.*, 84 (2000), 297-302
- 39 Yang H.H., Myung N.V., Yee J., Park D.Y., Yoo B.Y., Schwartz M., Nobe K., Judy J.W. – Ferromagnetic micromechanical magnetometer, *Sens. Act. A* 97-98 (2002), 88-97
- 40 Givens R.B., Murphy J.C., Osiander R., Kistenmacher T.J., Wickenden D.K. – A high sensitivity, wide dynamic range magnetometer designed on a xylophone resonator, *Appl. Phys. Lett.*, 69 m(1996), 2755-2757

Author: Sławomir Tumanski, professor of Warsaw University of Technology, Warsaw University of Tvechnology, IETiSIP, 00-661 Warsaw, Koszykowa 75, E-mail: slawomir.tumanski@ee.pw.edu.pl